Infrared Absorption and Electron Effective Mass in *n*-Type Gallium Arsenide

W. G. SPITZER AND J. M. WHELAN
Bell Telephone Laboratories, Murray Hill, New Jersey
(Received November 4, 1958)

The infrared absorption between 0.85 and 25 microns has been measured as a function of carrier concentration for *n*-type single-crystal gallium arsenide. The absorption in the 1- to 5-micron region is compatible with a model in which there are minima ~0.25 ev above the bottom of the conduction band. Infrared reflectivity measurements on several samples of different carrier concentrations were used to deduce the free-carrier contribution to the electric susceptibility and the electron effective mass. The results indicate a value for the mass of $(0.078\pm0.004)m$ with an indication of an increase for the sample of highest carrier concentration. This value is substantially larger than previously reported values.

I. INTRODUCTION

IN the few years that single-crystal material has been available, gallium arsenide has been the subject of considerable infrared investigation. The room-temperature energy gap obtained from optical data is 1.35 ev.[1] The infrared lattice absorption spectrum has been measured from the fundamental absorption edge at ~0.9 μ (micron) to 45 μ.[2] It has been shown that GaAs has an optically active fundamental lattice vibration at 36 μ.[3] Reflectivity measurements indicate a refractive index of 3.3[1] between 2 and 15 μ. The absorption spectrum of *p*-type GaAs,[4] similar to that of *p*-type germanium,[5] has 3 absorption bands which result from interband transitions within the valence band. Free-carrier absorption measurements of *n*-type GaAs have also been reported.[1] The absorption coefficient increases with increasing wavelength.

Callaway[6] has made use of second-order perturbation theory to relate the energy band structures of germanium and GaAs. His calculations indicate that the lowest minimum in the GaAs conduction band is probably at the center of the Brillouin zone ($\mathbf{k}=0$) with the minima in the [111] directions at a somewhat higher energy. The conduction electron effective mass has been measured by Barcus *et al.*[7] for a single GaAs specimen by using the optical method of Spitzer and Fan.[8] An effective mass $m^*=0.043m$ was obtained where m is the free-electron mass. Measurements of the effective mass from thermoelectric power have also been reported. Early results[1] gave $m^*\sim0.03m$ while later measurements[9] indicated $m^*\sim0.06m$. Magnetoresistance measurements[10] are compatible with spherical surfaces of constant energy which would indicate that the conduction band minimum is at $\mathbf{k}=0$.

The present measurements were made with a number of single-crystal *n*-type GaAs specimens. The measurements show that all of the samples have a free-carrier absorption which rises as λ^3 for wavelengths greater than 5 μ. Between the absorption edge and 5 μ, there is additional absorption which may be interpreted in terms of Callaway's model as due to electron transitions from the conduction band minimum at $\mathbf{k}=0$ to the minima in the [111] directions. Effective mass measurements were made with these same samples by using the technique of Spitzer and Fan. The effective mass obtained is $m^*=(0.078\pm0.004)m$ with an indication of a rise in m^* for the sample of highest carrier concentration.

II. SAMPLE PREPARATION

The GaAs specimens used in this work were cut from single-crystal material grown by the floating zone method.[11] Four of the six *n*-type crystals used were produced by intentionally doping with either selenium or tellurium. The impurity was introduced via the As atmosphere in which the crystals were grown. Bridge-shaped samples for Hall measurements were prepared from sections of the various crystals cut parallel to the growth axis. The samples for the optical measurements were also cut parallel to the axis of growth and adjacent to the Hall specimens. Both the electrical and optical measurements were made in corresponding regions with respect to the length of the crystal. Previous resistivity data and radioautographs of single crystals doped with a number of radioactive impurities have shown that the impurity distribution is uniform over the cross section perpendicular to the growth axis except for a layer $\sim5\times10^{-2}$mm deep near the periphery of the crystal.

III. EXPERIMENTAL RESULTS

A. Absorption

Table I is a list of the samples which were used for the optical measurements. The carrier concentration, n, was determined from the room-temperature Hall

[1] Barrie, Cunnell, Edmond, and Ross, Physica **20**, 1087 (1954); F. Oswald and R. Schade, Z. Naturforsch. **9a**, 611 (1954).
[2] H. Hrostowski and J. M. Whelan (to be published).
[3] Picus, Burstein, and Hennis, Bull. Am. Phys. Soc. Ser. II, **1**, 126 (1956).
[4] R. Braunstein, Bull. Am. Phys. Soc. Ser. II, **3**, 218 (1958).
[5] R. J. Collins and H. Y. Fan, Phys. Rev. **93**, 674 (1954); also H. B. Briggs and R. C. Fletcher, Phys. Rev. **91**, 1342 (1953).
[6] J. Callaway, J. Electronics **2**, 330 (1957).
[7] Barcus, Perlmutter, and Callaway, Bull. Am. Phys. Soc. Ser. II, **3**, 30 (1958); Phys. Rev. **111**, 167 (1958).
[8] W. G. Spitzer and H. Y. Fan, Phys. Rev. **106**, 882 (1957).
[9] Edmond, Broom, and Cunnell, *Rugby Semiconductor Conference* (The Physical Society, London, 1956).
[10] M. Glicksman, Bulletin of the International Conference on Semiconductors, Rochester, New York, 1958, p. 48 (unpublished).
[11] J. M. Whelan and G. H. Wheatley, J. Phys. Chem. Solids **6**, 169 (1958).

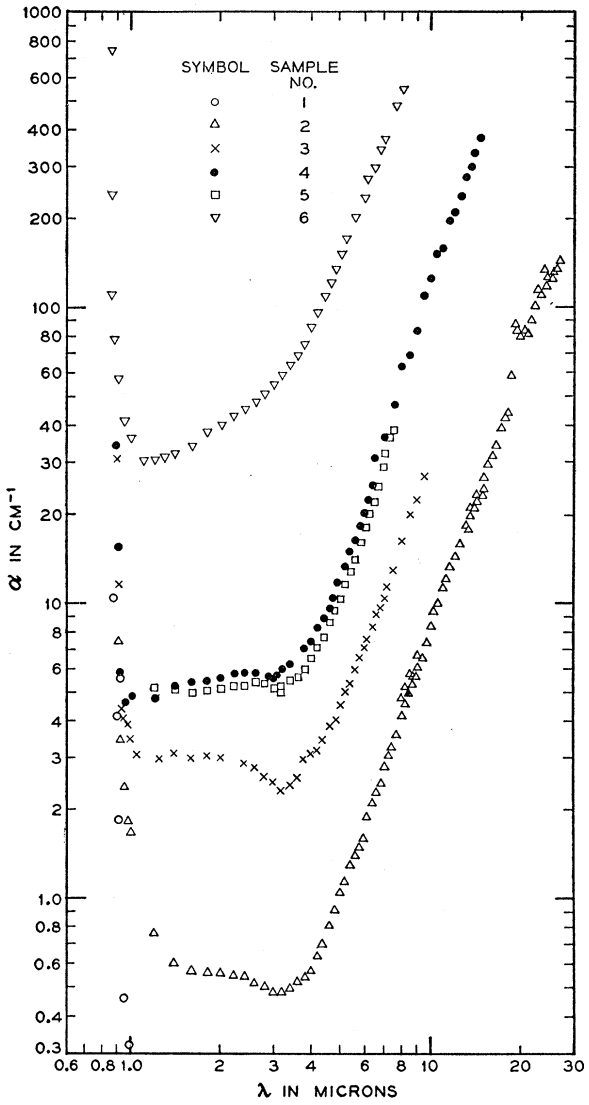

FIG. 1. Room-temperature absorption coefficient as of function of wavelength for the six samples in Table I.

coefficient. Since samples 2 through 6 vary from nearly degenerate to strongly degenerate, the relation $R_H=-1/ne$ was used. The second column indicates the chemical donor impurity in the crystal. The donor impurities of samples 1 and 3 are not known.

TABLE I. Electron concentration and doping impurities in GaAs samples used for optical measurements

Sample No.	Donor impurity	$n(\text{cm}^{-3})$
1	...	$\leq 5\times10^{14}$
2	Se	1.3×10^{17}
3	...	4.9×10^{17}
4	Se	1.09×10^{18}
5	Te	1.12×10^{18}
6	Se	5.4×10^{18}

Figure 1 gives the room-temperature absorption coefficient as a function of wavelength for the samples of Table I. The absorption coefficients were determined from the measured transmission T by using the expression[12]

$$T=(1-R)^2e^{-\alpha x}/(1-R^2e^{-2\alpha x}), \quad (1)$$

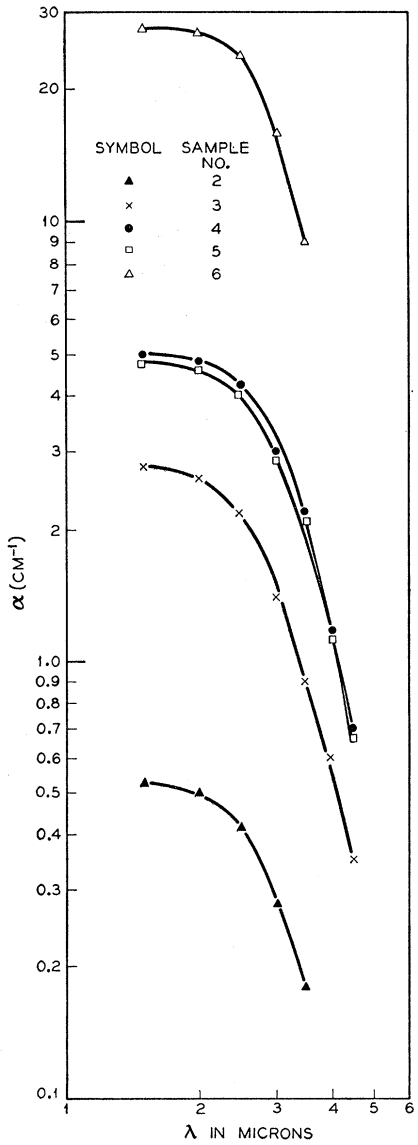

FIG. 2. Absorption coefficient *vs* wavelength for the additional absorption observed in the 1-5 μ region.

where x is the sample thickness, α is the absorption coefficient, and R is the reflectivity measured at the same wavelength as T. The absorption curves of Fig. 1 are very similar to those which have been reported for

[12] H. Y. Fan and M. Becker, in *Symposium Volume of the Reading Conference*, edited by H. K. Henisch (Butterworths Scientific Publications, Ltd., London, 1951).

n-type silicon.[13] For wavelengths $(\lambda)\gtrsim 5\ \mu$ the absorption curves of Fig. 1 rise smoothly with wavelength, which is characteristic of free-carrier absorption. The bands observed in Fig. 1 for $\lambda > 17\ \mu$ are due to absorption by the GaAs lattice. Between approximately 1.0 μ and 5 μ the curves are the result of the superposition of the normal free-carrier absorption seen at longer wavelengths and some additional absorption due to another mechanism. The spectral shape of this additional absorption may be obtained by extrapolating the free-carrier curve for $\lambda > 5\ \mu$ back to shorter wavelengths and subtracting from the measured data. The resulting curves are shown in Fig. 2. The long-wavelength threshold for this absorption is between 4.5 μ and 5.5 μ or (0.25 ± 0.03) ev. The absorption in Fig. 2 is proportional to the carrier concentration. This proportionality may be seen more clearly in Fig. 3 where the absorption coefficients for the samples of Fig. 2 are plotted as a function of the carrier concentration for both $\lambda = 2\ \mu$ and 3 μ. The points lie close to straight lines of slope 1.

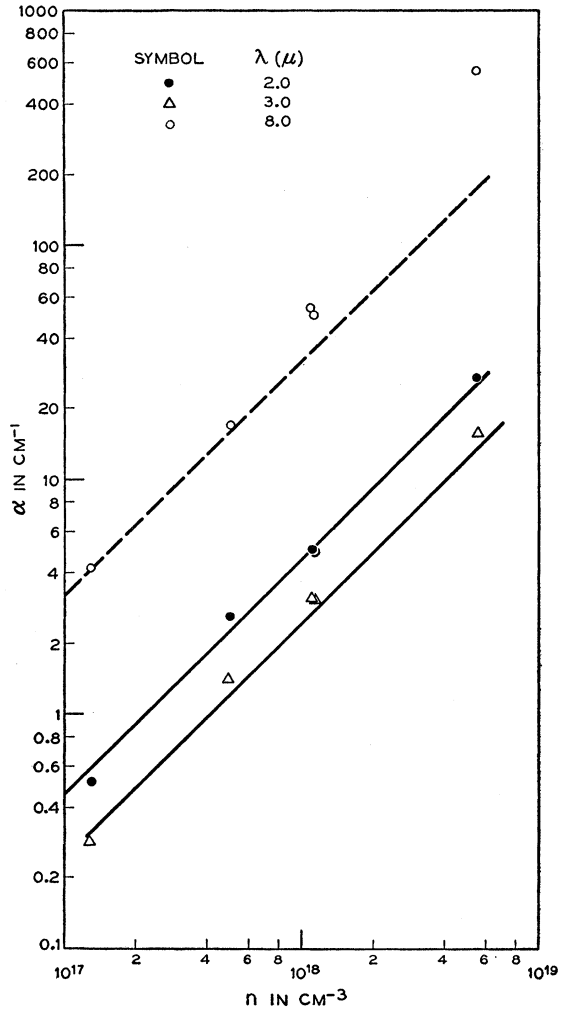

FIG. 3. Absorption coefficient as a function of carrier concentration at 2, 3, and 8 μ. The lines are drawn with a slope of unity.

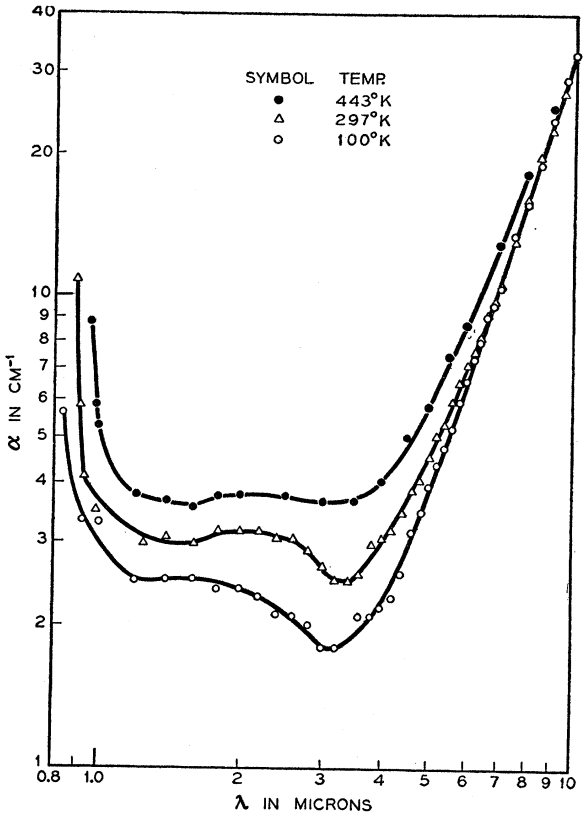

FIG. 4. Absorption vs wavelength for sample No. 3 at three different temperatures.

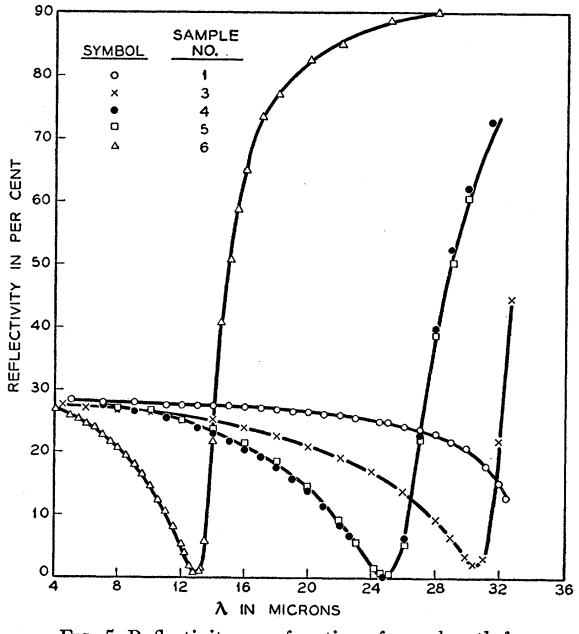

FIG. 5. Reflectivity as a function of wavelength for five samples in Table I.

[13] W. G. Spitzer and H. Y. Fan, Phys. Rev. **108**, 268 (1957).

Figure 4 gives the measured absorption coefficient for sample No. 3 as a function of wavelength for 3 different temperatures. The additional absorption in the 1 μ to 5 μ region shows little change with temperature.

The absorption coefficient of Fig. 1 for $\lambda > 5$ μ rises with close to a λ^3 dependence for all of the samples measured. The absorption in this wavelength region is not proportional to the carrier concentration as can be seen from Fig. 3. For $\lambda = 8$ μ the points do not lie close to a line of slope 1 (dashed line). The measured absorption increases more rapidly than the carrier concentration.

B. Effective Mass

Figure 5 gives the reflectivity as a function of wavelength for samples Nos. 1, 3, 4, 5, and 6. The decrease in the reflectivity of the pure sample (No. 1) at the longest wavelengths is due to the fundamental lattice band at 36 μ. The electric susceptibility arising from this band is negative for $\lambda < 36$ μ, resulting in a decrease of the refractive index and hence the reflectivity. The impure samples (Nos. 3, 4, 5, and 6) show a much stronger dependence of the reflectivity on wavelength. This behavior has been shown[8] to be the result of the influence of the free carriers on the dielectric constant. The electric susceptibility of the free carriers, χ_c, has been calculated for these four samples according to the procedure of Spitzer and Fan and is given in Fig. 6. As theory predicts, $-4\pi\chi_c$ is proportional to λ^2. The values of m^* obtained from Fig. 6 with the expression

$$\chi_c = -ne^2/\omega^2 m^* \qquad (2)$$

are $0.078m$ for sample No. 3, $0.079m$ for samples No. 4 and 5, and $0.089m$ for sample No. 6. In cases where the reflectivity has a very deep minimum the effective mass may be quickly estimated with the aid of the expression

$$m^* \simeq 4\pi ne^2/[4\pi^2\nu_{\min}^2(\epsilon_0 - 1)], \qquad (3)$$

where $\nu_{\min}$ is the frequency of the reflectivity minimum, ϵ_0 is the dielectric constant of the pure material at $\nu_{\min}$, and n is the carrier concentration. This expression is readily obtained from reference 10 under the conditions that the refractive index is $\simeq 1$ and the extinction coefficient is $\simeq 0$. Using (3) and the values of $\nu_{\min}$ from Fig. 5, the values of m^* are $0.079m$ for sample No. 3, $0.079m$ for samples Nos. 4 and 5, and $0.086m$ for sample No. 6.

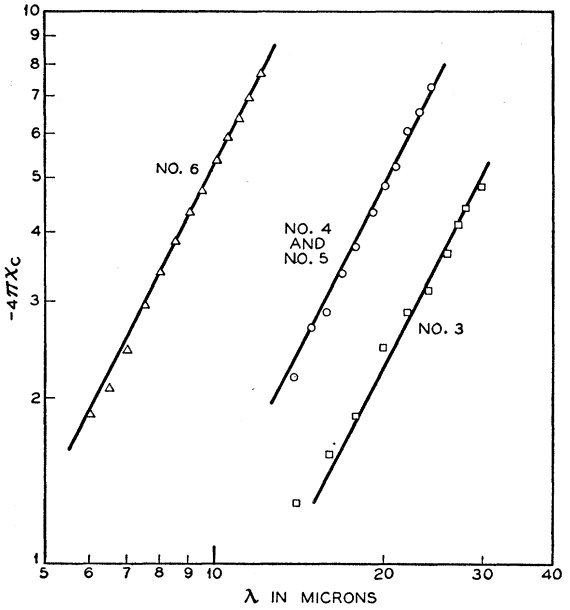

FIG. 6. Electric susceptibility *vs* wavelength for the samples in Fig. 5. The solid lines indicate a λ^2 dependence.

IV. DISCUSSION

The absorption observed in the 1 μ to 5 μ region has been regarded as the addition of the normal conductive free-carrier absorption and some additional absorption. As in the case of n-type silicon, there are at least two possible explanations for the additional absorption. The absorption could arise from the excitation of electrons to the conduction band from deep lying levels within the forbidden energy gap. However, since different donor impurities were used in the specimens and and since the absorption coefficient is proportional to the carrier concentration, this explanation is unlikely. A more likely explanation is that the absorption is due to the excitation of electrons from the conduction band minimum to a higher lying minimum (or minima). From the conduction band model proposed by Callaway, the electron transitions could be from $\mathbf{k}=0$ minimum to the minima in the [111] directions. If this is the case then the energy separation between these two minima is about 0.25 ev. Since for the more impure samples the Fermi level is above the conduction band minimum the low-energy threshold of Fig. 2 should shift to still lower energy with increasing carrier concentration. However the values of α in Fig. 2 for this energy region are obtained by subtracting two nearly equal quantities and hence very inaccurate. Gray and Ehrenreich[14] have offered a possible explanation for a maximum observed in the temperature dependence of the Hall coefficient of n-type GaAs by using the type of conduction band structure proposed by Callaway. The energy separation for the two minima required to fit the Hall measurements is between 0.2 and 0.4 ev, which is in agreement with the 0.25-ev value found here.

The effective mass obtained here should be that of the $\mathbf{k}=0$ minimum. Our value of nearly $0.08m$ differs by a factor of approximately 2 from that reported by Barcus[7] for a single polycrystalline specimen. With an effective mass of $0.08m$ and a degree of ionicity estimated from the reflectivity data of Picus,[15] Ehrenreich[16]

[14] P. V. Gray and H. Ehrenreich, Bull. Am. Phys. Soc. Ser. II, 3, 255 (1958).
[15] Picus, Burstein, Hass, and Henvis, J. Phys. Chem. Solids (to be published).
[16] H. Ehrenreich (private communication).

has calculated the electron mobility for polar lattice scattering. The calculated room-temperature mobility is 7000 cm²/volt sec which is in reasonable agreement with experimental values for the purest samples.[11]

The λ^3 dependence of the absorption coefficient at longer wavelengths is similar to that which has been reported for n-type InAs.[17] The dependence of the absorption on carrier concentration indicates the probable presence of some impurity-scattering absorption.[18] The λ^3 dependence of the absorption is close to that which is theoretically predicted by Fan[18] and by Meyer[19] for impurity-scattering absorption. However, at the present time, theoretical calculations have not been made for the spectral shape of the lattice-scattering absorption in partially polar semiconductors.

ACKNOWLEDGMENTS

The authors wish to express their appreciation to Mr. G. Sorin who aided in some of the infrared measurements and Mr. J. A. Ditzenberger who assisted in the preparation of some of the crystals. We are also indebted to Dr. D. A. Kleinman and Dr. H. Ehrenreich for several interesting discussions on this work.

[17] J. R. Dixon and D. P. Enright, Bull Am. Phys. Soc. Ser. II, 3, 255 (1958).
[18] Fan, Spitzer, and Collins, Phys. Rev. **101**, 566 (1956).
[19] H. J. G. Meyer, Phys. Rev. **112**, 298 (1958).

PHYSICAL REVIEW VOLUME 114, NUMBER 1 APRIL 1, 1959

Study of Ferroelectric Transitions of Solid-Solution Single Crystals of $KNbO_3$-$KTaO_3$

S. TRIEBWASSER
International Business Machines Corporation, Poughkeepsie, New York
(Received November 13, 1958)

Methods of preparation and results of measurements of the dielectric constant of solid-solution single crystals of $KNbO_3$ and $KTaO_3$ are presented. Data are given for the composition range 0–80 mole percent $KTaO_3$ in the temperature interval −180°C to 450°C. It is found that all of the crystals studied show Curie-law behavior of the dielectric constant in the paraelectric state. The data indicate that the paraelectric to ferroelectric transition, which is first order for pure $KNbO_3$, becomes second order at a concentration of approximately 55 mole percent $KTaO_3$. Analysis of the results in terms of Slater's model of ferroelectricity in a perovskite lattice leads to the conclusion that the dependence of the Lorentz correction on volume plays a major role in determining the ferroelectric behavior. Ionic polarizabilities and their dependence on volume are also discussed.

I. INTRODUCTION

At the present time, more than ten years after the discovery of ferroelectricity in $BaTiO_3$, a large body of data has been accumulated not only on this perovskite-type crystal, but on several others, both ferroelectric and antiferroelectric in behavior. The reader is referred to Kaenzig's[1] excellent review of the subject which lists many references. The experimental data has been described and explained rather successfully by a phenomenological theory developed in some detail be Devonshire.[2] Slater[3] extended this theory and showed how the observed dependence of the free energy on temperature and electric polarization could be derived accurately from a consideration of the ionic structure of the lattice and the calculated internal Lorentz field. Further examination of Slater's model by this author[4] indicated that the important details of the experimental facts could be predicted at least qualitatively by improving the model somewhat. The present state of the theory is such as to provide order of magnitude agreement with the observed data, but in view of present uncertainties of the details of the bonding structure and short range interactions of the atoms in the lattice it appears that quantitative explanations cannot be made.

The present study was motivated by a desire to study the effect of the variation of a structural parameter in a perovskite ferroelectric. $KNbO_3$ is a ferroelectric exhibiting a transition from a cubic paraelectric to tetragonal ferroelectric state at ~700°K.[5] $KTaO_3$ has a transition, structural details of which are not known at present, from paraelectric to ferroelectric state at 13°K.[6] At 450°C, a temperature at which both materials are cubic, the lattice parameter of $KNbO_3$ is 4.0226 A while for $KTaO_3$ it is 4.0026 A.[7] It was felt that solid solutions of these two components would generate a lattice in which the structural perturbations would be

[1] W. Kaenzig, in *Solid State Physics*, edited by F. Seitz and D. Turnbull (Academic Press, Inc., New York, 1957), Vol. 4.
[2] A. F. Devonshire, Phil. Mag. **40**, 1040 (1949).
[3] J. C. Slater, Phys. Rev. **78**, 748 (1950).
[4] S. Triebwasser, J. Phys. Chem. Solids **3**, 53 (1957).
[5] B. T. Matthias and J. P. Remeika, Phys. Rev. **82**, 727 (1951).
[6] Hulm, Matthias, and Long, Phys. Rev. **79**, 885 (1950).
[7] M. Berry and F. Holtzberg (private communication).